

3. COMPARATIVE BRAKING PERFORMANCE OF VARIOUS AIRCRAFT ON GROOVED AND UNGROOVED PAVEMENTS AT THE LANDING RESEARCH RUNWAY, NASA WOLLOPS STATION

By Thomas J. Yager
NASA Langley Research Center

SUMMARY

The transverse groove configuration of 1 in. \times $\frac{1}{4}$ in. \times $\frac{1}{4}$ in. installed at the landing research runway at NASA Wallops Station for full-scale aircraft test evaluation was selected on the basis of aircraft tire traction tests conducted at the Langley landing-loads track on 19 different transversely grooved test surfaces. In order to provide the reader some background for the full-scale aircraft tests, some of the test results obtained at the track are presented and discussed. These results indicate that grooved pavements offer great promise for increasing aircraft ground performance during landing and take-off operations under adverse conditions. Also discussed are the comparative aircraft braking test data obtained on similar grooved and ungrooved surfaces at the landing research runway with a fully instrumented McDonnell Douglas F-4D jet fighter aircraft and the Convair 990 4-engine jet transport aircraft. The aircraft test results substantiate and supplement the track data and indicate that transverse runway grooves provide greatly increased aircraft braking and steering capability for wet, flooded, and slush-covered runway surfaces.

INTRODUCTION

In order to provide the reader some background for the full-scale aircraft tests on the transversely grooved landing research runway at NASA Wallops Station, some test results obtained during aircraft tire braking tests on several different grooved and ungrooved surfaces at the Langley landing-loads track are discussed. The purpose of the evaluation at the track was to determine which groove configuration, out of 19 configurations tested, offered the best aircraft tire braking capability; on the basis of these test results, the 1-in. \times $\frac{1}{4}$ -in. \times $\frac{1}{4}$ -in. groove configuration was selected.

Having obtained very promising test results at the Langley landing-loads track on the effects of transverse pavement grooving as a means of improving aircraft tire traction capability and recognizing the limitations of the landing-loads track, a search was initiated in late 1966 for a suitable test runway for use in making similar tests on full-scale aircraft. Runway 4/22 at NASA Wallops Station was selected, with test surface modification work (including installation of the selected groove configuration) being

completed in late 1967. Full-scale aircraft tests to determine the effects of grooved runway surfaces on aircraft landing and take-off operations under dry, wet, flooded, and slush-covered conditions were started in February 1968.

The aircraft braking test results obtained on the landing research runway at NASA Wallops Station during nearly 200 test runs with an F-4D jet fighter and the 990 4-engine jet transport are presented and discussed. These comparative aircraft test results on grooved and ungrooved surfaces for dry, wet, flooded, and slush-covered conditions substantiate and supplement the test results obtained earlier at the landing-loads track.

PAVEMENT GROOVING EVALUATION AT THE LANDING-LOADS TRACK

Test Equipment and Procedure

The pavement grooving evaluation was conducted at the Langley landing-loads track by using the large test carriage. The test tire fixture, mounted in the center of the carriage, is instrumented to measure the loads developed by the tire during a test run at speeds up to 100 knots. References 1 and 2 give a more detailed description of the equipment and operation of the track. Excellent repeatability of test conditions can be obtained with this equipment, and by means of an 18-channel oscillograph recorder, complete time histories of tire performance during a test run were recorded for data evaluation. The five different aircraft tires used in this investigation varied in size and tread design from a smooth, fabric-reinforced rubber tread, type VIII, 27.5×7.5 tire to a 7-groove, all rubber tread, type VII, 49×17 tire. The transversely grooved test surfaces were constructed of removable, precast concrete strips, 10 ft in length, which were frozen in place in the 200-ft-long brine pipe section of the track normally used to obtain an ice test surface. Photographs and a plan drawing of these precast concrete test strips are shown in figure 1. A minimum test-surface length of 20 ft (two concrete strips placed end to end) was used during actual test runs in addition to the permanent concrete and asphalt surfaces located in the remaining 1000 ft of the track test section. With this surface arrangement a maximum of 10 different grooved surfaces could be evaluated and compared to the permanent ungrooved surfaces during each test run. Two concrete test strips were also left ungrooved for comparing and evaluating tire performance on the grooved surfaces. The various groove configurations were sawed or flailed into each of these concrete strips prior to installation.

The values of groove pitch and width for the configurations tested are given in the following table:

Groove width, in.	Groove pitch, in.		
$\frac{1}{8}$	1	$1\frac{1}{2}$	2
$\frac{1}{4}$	1	$1\frac{1}{2}$	2
$\frac{3}{8}$	1	$1\frac{1}{2}$	2

Each of these configurations was tested for groove depths of 1/8 in. and 1/4 in. which resulted in test data being obtained on 18 different groove configurations. The 1/8-in.-deep grooves were cut with a flailing tool which resulted in rounded corners at the top and bottom edges of these grooves. The 1/4-in.-deep grooves were cut with a saw which resulted in relatively sharp corners.

As a means of determining the optimum groove configurations of those considered in this study, tests were conducted to evaluate the effect of transversely grooved pavement surfaces on aircraft tire performance; namely, (1) rolling resistance, (2) cornering capability, and (3) braking effectiveness. Additional tests were conducted to determine the effect of freeze-thaw cycles on grooved pavement surfaces. Although all the test results obtained from the pavement grooving evaluation are not given herein, the general data trends which were established during the investigation are presented.

Test Results

Aircraft tire rolling resistance.- Rolling resistance coefficient values were obtained with a smooth, fabric-reinforced rubber tread, type VIII, 27.5 × 7.5 tire inflated to 400 lb/in². Tests were made at 4° yaw on various surfaces for both flooded and damp conditions, and the results are shown in figure 2 as a function of ground speed. The solid line is faired through the ungrooved concrete test strip results and used for comparison with the results obtained on the other test surfaces. The surface roughness or texture of the three ungrooved test surfaces shown in figure 2 varied from an average texture depth (see refs. 3 and 4) of 0.04 mm for the smooth concrete to 0.32 mm for the float-finished concrete. The ungrooved concrete test strip had an average texture depth of 0.15 mm. With the pavement surface under flooded conditions (water depth varied from 0.2 to 0.3 in.), the rolling resistance coefficient of the smooth 27.5 × 7.5 test tire increases with speed but the data indicate no significant difference in the values obtained on the ungrooved concrete from those obtained on the other test surfaces. For damp conditions with no standing water on the surfaces, the rolling resistance values obtained on the ungrooved surface remain constant between 0.03 and 0.04 with increasing forward velocity. Less deviation from the tire rolling resistance coefficient values for the

ungrooved surface was obtained on the other grooved test surfaces not shown in figure 2. The results of these unbraked tire tests indicate that transversely grooved pavement surfaces do not significantly affect tire rolling resistance.

Aircraft tire cornering capability. - The effect of pavement surface configuration on the side or cornering force developed by the smooth 27.5×7.5 type VIII tire operated at 4° yaw is shown in figure 3. In this figure the cornering force obtained for each particular surface configuration is divided by the cornering force value obtained under the same conditions on the dry ungrooved surface. This value is then multiplied by 100 to express it as percent of dry ungrooved cornering force. The percent of dry ungrooved cornering force is plotted against the velocity ratio which is the actual ground speed divided by the computed critical hydroplaning speed. (See ref. 5.) A velocity ratio of 1 for the test conditions shown in figure 3 is equal to a ground speed of 180 knots. Comparative data are presented for three ungrooved test surfaces, nine sawed groove configurations, and seven flailed groove configurations for both flooded (water depth varied from 0.2 to 0.3 in.) and damp conditions. Data were not obtained on the flailed groove configurations of $1\frac{1}{2}$ in. \times $\frac{1}{8}$ in. \times $\frac{1}{8}$ in. and 2 in. \times $\frac{1}{8}$ in. \times $\frac{1}{8}$ in. with the smooth 27.5×7.5 test tire.

In general, the data show that a greater percent of the dry ungrooved surface cornering force was obtained on the damp test surfaces as compared to that obtained for flooded conditions. For similar surface wetness conditions, the data obtained on the ungrooved test surfaces are significantly lower than the data obtained on the sawed-groove and flailed-groove test surfaces. However, the degradation in tire cornering force developed on the sawed-groove test surfaces for flooded conditions is substantially less than that for the damp surface condition, particularly at the higher, more critical speeds. A greater degradation in tire cornering force is shown by the data obtained on the ungrooved and flailed-groove test surfaces for flooded conditions compared to the data obtained for damp conditions.

The percent of dry ungrooved surface cornering force data shown in figure 3 also indicate the effect of groove spacing and groove width on tire cornering force. By increasing the spacing between the grooves from 1 in. to 2 in., a proportionately lower percent of dry ungrooved surface cornering force was developed at the higher test speeds. Increasing the groove widths from $\frac{1}{8}$ in. to $\frac{3}{8}$ in., however, did not result in proportionately higher tire cornering traction for the critical flooded surface condition. The data in figure 3 show that under flooded conditions the sawed groove configuration of 1 in. \times $\frac{1}{4}$ in. \times $\frac{1}{4}$ in. maintained the greatest percent of dry ungrooved surface cornering force throughout the test speed range.

Aircraft tire braking effectiveness. - Previous tire traction research has shown that tire braking capability reaches a peak or maximum value at a slip ratio which depends primarily on the tire elastic properties and the maximum available coefficient

of friction. A slip ratio of 0 corresponds to the free-rolling condition and a slip ratio of 1 corresponds to the locked-wheel or full-skid condition (ref. 6). As the tire is allowed to spin down from this peak braking friction condition, tire braking capability is significantly reduced and tire side force or steering capability is also reduced. For the locked-wheel condition the side force is reduced to zero. Data showing the variation of skidding friction coefficient values obtained on the three principal types of surfaces tested are shown in figure 4 as a function of velocity ratio. These data were obtained with the smooth 27.5×7.5 tire operated at 4° yaw and for flooded (water depth varied from 0.2 to 0.3 in.) surface conditions. In general, the locked-wheel friction coefficient data obtained on both the sawed- and flaired-groove surfaces are significantly higher than the data obtained on the ungrooved concrete test surface throughout the test speed range. However, as speed is increased, there is a rapid reduction in the locked-wheel friction coefficient obtained on the ungrooved and flaired-groove test surfaces. On the sawed-groove test surfaces, a high level of locked-wheel friction coefficient is maintained throughout the test speed range. As the data shown in figure 4 indicate, the highest level of locked-wheel friction coefficient was maintained on the sawed $1\text{-in.} \times \frac{1}{4}\text{-in.} \times \frac{1}{4}\text{-in.}$ groove configuration.

In addition to these comparative tests to determine the optimum of the various groove configurations, the effect of alternately freezing and thawing several flooded grooved pavement surfaces was studied. Since the grooved concrete test strips were frozen in place during the aircraft tire test runs, it was a simple matter to add additional water to a depth slightly greater than the surface of the groove lands. Complete freezing was accomplished overnight by the refrigeration system. The solid ice formation on top of the grooved surfaces was then quickly thawed by means of a water hose, and several low-speed (4 knots) locked-wheel braking test runs were conducted before adding water to freeze the surfaces again. In this manner, the grooved test surfaces were subjected to 22 freeze-thaw cycles. As shown in figure 5, the 22 freeze-thaw cycles did not have a significant effect on the locked-wheel friction coefficient developed by a 3-groove, fabric-reinforced rubber tread, type VIII, $30 \times 11.5\text{-}14.5$ tire on a $1\text{-in.} \times \frac{1}{4}\text{-in.} \times \frac{1}{8}\text{-in.}$ grooved surface and a $1\text{-in.} \times \frac{1}{8}\text{-in.} \times \frac{1}{8}\text{-in.}$ grooved surface for flooded conditions. Between each of the freeze-thaw cycles, closeup photographs of the grooved test surface, as well as silicone rubber molds, were taken in the area of the test tire path. No significant change or deterioration of the grooved surfaces was found during the process of being subjected to not only 22 freeze-thaw cycles but nearly 50 low-speed locked-wheel braking tests.

SUMMARY OF RESULTS OBTAINED FROM STUDIES OF VARIOUS GROOVE CONFIGURATIONS

Test results were obtained during the evaluation of various groove configurations by use of a variety of aircraft tires at the Langley landing-loads track. Comparison of data from these grooved surfaces and from similar ungrooved concrete surfaces under the same test conditions indicates that pavement grooving results in

- (1) No significant increase in aircraft tire rolling resistance
- (2) Substantial improvement in aircraft tire cornering force or steering capability
- (3) Greatly improved aircraft tire braking capability

On the basis of aircraft tire traction performance on flooded surfaces at speeds up to 100 knots, the 1-in. \times $\frac{1}{4}$ -in. \times $\frac{1}{4}$ -in. sawed groove configuration was determined to be better than the other groove configurations tested. During all the yawed rolling and braking test runs and during the 22 alternate freeze-thaw cycles, no significant surface deterioration of the groove configurations was observed.

AIRCRAFT TEST EVALUATION AT THE LANDING RESEARCH RUNWAY

Test Procedure

Nearly 200 test runs with an F-4D jet fighter and the 990 4-engine jet transport have been made on the landing research runway at NASA Wallops Station. With the data obtained from these two fully instrumented test aircraft, several factors affecting aircraft ground performance were evaluated. On similar grooved and ungrooved surfaces, comparative free-rolling touch-and-go type tests as well as accelerate-stop type maximum antiskid braking test runs were made at ground speeds up to 150 knots for dry, wet, flooded, and slush-covered surface conditions. In comparing the F-4D and 990 aircraft braking performance, the effects of runway surface grooves, tire tread design, and anti-skid braking systems on aircraft braking and directional control were studied. The different configurations of the main-wheel landing gears on the two aircraft were also considered in this investigation.

A schematic view of the landing research runway indicating the nine different test surfaces is shown in figure 6. The overall dimensions of the runway are 8750 ft by 150 ft with the 3450-ft by 50-ft test section located in the middle. A level (both transversely and longitudinally) 1400-ft concrete section and a 1400-ft asphalt section are separated by a 650-ft Gripstop transition surface (see ref. 7) having a longitudinal slope of 0.1 percent. The terms "smooth" and "textured" used in figure 6 indicate the relative roughness

of the test-surface finishes. Half of each of the four 700-ft concrete and asphalt sections having different surface finishes is transversely grooved so that comparative aircraft tire traction values could be obtained on grooved and ungrooved sections of the same pavement. The groove configuration is 1 in. \times $\frac{1}{4}$ in. \times $\frac{1}{4}$ in. The surface code letters A to I are used to identify the test surface, as follows:

Surface A	Canvas-belt drag finished concrete, ungrooved
Surface B	Canvas-belt drag finished concrete, grooved
Surface C	Burlap drag finished concrete, grooved
Surface D	Burlap drag finished concrete, ungrooved
Surface E	Gripstop transition surface
Surface F	Small-aggregate asphalt, ungrooved
Surface G	Small-aggregate asphalt, grooved
Surface H	Large-aggregate asphalt, grooved
Surface I	Large-aggregate asphalt, ungrooved

A detailed description of these test surfaces is given in reference 7.

The two different wetness conditions used on the surfaces of the landing research runway during the aircraft tests are shown in figure 7. In attempting to obtain a wet condition with a runway surface water depth of less than 0.1 in., some surface water collected in surface depressions to form isolated puddles. For the flooded surface condition, numerous water-depth measurements were taken before each test run on the runway center line and on each side in the main-gear wheel path area of the test aircraft to establish a surface water-depth profile. As a result of wind effects on the surface water during the aircraft test runs, some areas of the test surface were damp and other areas had a water depth greater than 0.3 in. For the flooded surface condition, however, the aircraft braking test data evaluation was confined to the test-surface area having a water depth between 0.1 and 0.3 in.

From aerial photographs of the wet test surfaces with isolated puddles, similar to the one shown in figure 8, the effect of runway grooves on water drainage is indicated. The two wet test surfaces shown in the photograph (fig. 8) are grooved and ungrooved asphalt. Although the same amount of water has been applied to both test surfaces, the ungrooved surface has a thin water film (as indicated by the light reflection in the photograph) but the water on the grooved surface has drained into the pavement grooves, resulting in only isolated puddles and no significant water film. It is apparent that the grooved pavement is faster draining than the ungrooved pavement for the same wetness condition.

Test Instrumentation and Data

By means of 36-channel oscillograph recorders, shown in figure 9, complete time histories of aircraft ground performance during a test run were recorded for data evaluation. Individual aircraft wheel velocity, brake pressure, and antiskid valve action as well as variations in engine speed and in nose- and main-gear strut pressure were monitored by the onboard instrumentation. Since most of the aircraft test runs were conducted at idle thrust and maximum braking conditions, variations in the F-4D brake pedal pressure metering valve were monitored and during the 990 aircraft tests the brake pedal positions were recorded. An instrument package (fig. 9), consisting of longitudinal, lateral, and normal accelerometers, pitch angle indicators, yaw attitude indicator, and a vertical gyro, was located at the center of gravity of the test aircraft. Location of the aircraft on the test section during a run was recorded by means of an event marker activated by the instrument man on board the aircraft during the test. By means of a wheel velocity gauge in the cockpit calibrated to true aircraft ground speed, the pilot could obtain the desired test-section entrance speed just prior to brake application. With the recorded data and data from a series of tare runs made throughout the test speed range of the aircraft to determine aerodynamic lift and drag coefficients, aircraft braking performance could be evaluated.

Some examples of the oscillograph traces obtained during tests of the F-4D and 990 aircraft are shown in figures 10 to 13. The data shown in these figures were obtained on the same grooved and ungrooved concrete test surfaces. It should be noted that the F-4D brake pedal pressure metering valve traces have been faired in figures 10 and 11. During both the F-4D and 990 aircraft braking tests the longitudinal accelerometer traces indicate a significant improvement in aircraft deceleration or braking effectiveness on the grooved concrete surface for both wetness conditions when compared with the low deceleration level obtained on the ungrooved concrete under similar test conditions. At a relatively high initial ground speed V of 107.5 knots, the longitudinal accelerometer trace recorded during a 990 aircraft braking test (fig. 12) indicates no significant difference in aircraft braking effectiveness on a dry grooved surface and a wet grooved surface with isolated puddles. From the wheel velocity traces shown in figures 10 to 13, complete wheel lockups did not occur during the F-4D aircraft braking tests but numerous multiple wheel spin-downs and complete wheel lockups occurred during the 990 braking tests on the ungrooved surfaces. On the grooved surfaces, only front wheel lockups occurred for flooded conditions during the 990 aircraft braking tests. This difference in wheel tire behavior during the F-4D and 990 braking tests could be attributed to differences in antiskid braking system characteristics and main-landing-gear configurations.

Test Results

With the initial test conditions for each of the aircraft braking test runs established and recorded, the oscillograph data reduction resulted in a time history profile of aircraft braking friction coefficients and ground speeds obtained throughout the assigned test surfaces at idle aircraft engine thrust. The computer data-reduction program considered corrections for aerodynamic lift and drag, wind direction and velocity, and ambient temperature and pressure. The aircraft braking friction coefficient data presented includes fluid impingement drag and slush drag on the aircraft.

Effects of runway grooves.- Comparative F-4D and 990 aircraft faired braking coefficient levels obtained at ground speeds up to 135 knots on grooved and ungrooved test surfaces for the wet and the flooded conditions are shown in figures 14 to 19. The F-4D aircraft braking data (figs. 14 and 15) were obtained with 3-groove fabric-reinforced rubber tread, type VIII, 30 × 11.5-14.5 main-gear tires. The 990 aircraft braking data (figs. 16 to 19) were obtained with 5-groove and smooth, all rubber retread, type VIII, 41 × 15.0-18 main-gear tires. The data obtained for flooded conditions are shown in figures 15, 17, and 19, but aircraft test time did not permit a complete evaluation of nine different runway surfaces. The dry braking friction coefficient curve was established from data obtained on several different dry grooved and ungrooved surfaces. Although there is a difference in the dry braking data curves for the F-4D aircraft and 990 aircraft, changes in runway surface configuration and tire tread design did not significantly affect the dry braking friction coefficient level obtained with each of the test aircraft.

For both wetness conditions shown in figures 14 to 19, the F-4D and 990 aircraft braking friction coefficient levels obtained on the grooved runway surfaces are substantially higher than those obtained on the similar ungrooved surfaces throughout the test speed range. The variation in aircraft braking data obtained on the five ungrooved surfaces under the wet condition with isolated puddles can be attributed to differences in runway surface texture or roughness as well as to surface texture type or configuration. By using the grease technique described in reference 4, the average runway surface texture depth was measured on the runway center line and varied as follows: 0.12 mm on surface A, 0.20 mm on surface D, 0.14 mm on surface E, 0.19 mm on surface F, and 0.32 mm on surface I.

In comparing the F-4D and 990 aircraft braking traction data obtained under similar test conditions, some of the differences in aircraft braking friction coefficient μ levels can be attributed to differences in antiskid braking system characteristics, landing gear response to runway roughness, and main-landing-gear wheel configurations. Although both aircraft antiskid braking systems reduce brake pressure when a critical wheel deceleration is reached, the antiskid braking system on the F-4D aircraft reduces brake pressure on both main wheels but the system on the 990 aircraft reduces brake

pressure on only the wheel or wheels operating at slip ratios beyond the peak of the μ -slip curve. Furthermore, the 990 aircraft has nose-wheel braking, whereas the F-4D has no brakes on the nose wheels. Considering the effects of the single main wheels of the F-4D main landing gear and the 4-wheel tandem bogie configuration of the 990 main landing gear, the forward pair of main-gear tires on the 990 aircraft displaces the runway surface water and enables the rear tires to maintain higher traction, particularly for flooded conditions.

In order to determine the effect of runway grooves on aircraft braking performance, an attempt was made to normalize these differences in aircraft antiskid braking system characteristics, main-landing-gear wheel configurations, and main-gear tire inflation pressures. In figure 20, the variation in the effective braking ratio (i.e., μ_{wet} divided by μ_{dry}) obtained with the F-4D and 990 aircraft on ungrooved and grooved asphalt (surfaces F and G) for wet conditions with isolated puddles is shown as a function of the ground velocity ratio. The 990 aircraft data were obtained with 5-groove rib-tread main-gear tires inflated to 160 lb/in² and the F-4D aircraft data were obtained with 3-groove rib-tread main-gear tires inflated to 280 lb/in². With these tire inflation pressures, the computed critical hydroplaning speed of the 990 and F-4D aircraft is 114 knots and 150 knots, respectively. In figure 20, the braking data obtained on the wet grooved asphalt with both aircraft throughout the speed range show very little reduction in aircraft braking effectiveness from the data obtained for a dry condition. On the wet ungrooved asphalt, the braking effectiveness of both airplanes reduces rapidly with increased speed to values between 20 and 30 percent of dry braking at a ground velocity ratio of 1 which represents the critical hydroplaning speeds of the two test aircraft. These test results, which are similar to the aircraft braking data obtained on the other test surfaces, indicate that runway grooves provide a substantial improvement in aircraft braking capability for wet conditions.

For a flooded condition on the same surfaces, figure 21 shows that the braking effectiveness of the two test aircraft reduces with speed on the grooved asphalt but there is a significant improvement compared with that obtained on the flooded ungrooved asphalt surface. The 990 aircraft maintained 65 percent of its dry braking capability on the flooded grooved asphalt at the calculated hydroplaning speed, but only achieved 20 percent on the flooded ungrooved asphalt. The F-4D aircraft maintained 35 percent of its dry braking capability on the flooded grooved asphalt at the calculated hydroplaning speed but on the flooded ungrooved asphalt, the braking effectiveness of the F-4D was completely lost.

During the 990 aircraft test program the effect of runway grooves on aircraft braking performance for a slush-covered surface condition was also evaluated. A 50-ft-wide by 600-ft-long slush bed on grooved and ungrooved concrete (surfaces C and D) was

prepared early in the morning by feeding 50 tons of ice in the form of 300-lb cakes into ice crusher-slinger machines and spraying the resulting snow-ice mixture onto the runway. The slush test bed which resulted from this operation is shown in figure 22. In order to expedite the application of the snow-ice mixture and achieve a uniform slush-bed consistency, four ice crusher-slinger machines were used, with two machines starting on each side of the test bed at the midpoint. As the snow-ice spraying operation progressed, the two machines on each side of the test bed moved apart until the desired test bed length, width, and depth were obtained. The snow-ice sprayed on the test surface was uniformly leveled and allowed to melt into the ice-water consistency of slush. Just prior to the initial aircraft test run, 12 samples were taken by using the method described in reference 8 to determine the average depth and specific gravity of the slush. The average slush depth on the runway test surfaces was 0.5 in. with an average specific gravity of 0.83.

For this slush-covered condition, the 990 aircraft braking performance data obtained on grooved and ungrooved concrete (surfaces C and D) are shown in figure 23. For comparison, effective braking ratios obtained for the wet condition with isolated puddles and for the flooded condition are also shown as a function of the ground velocity ratio. Significant improvement in 990 aircraft braking capability throughout the test speed range is indicated by comparison of the data obtained on the grooved concrete test surface with the data obtained on the similar ungrooved surface for the wet, flooded, and slush-covered conditions. The increase in effective braking ratio on the slush-covered ungrooved concrete surface as the aircraft approached the critical hydroplaning speed of 114 knots is a result of the buildup in slush spray impingement drag on the 990 aircraft. This slush drag on the aircraft decreases at or above critical hydroplaning speed on the ungrooved surface because the tires are displacing less slush from the runway. Similar aircraft braking test results on slush-covered ungrooved surfaces were obtained during the joint FAA-NASA slush tests with the 880 aircraft discussed in reference 8.

During the 990 aircraft braking tests on the slush-covered surfaces, the improvement in aircraft directional control provided by runway grooves was also demonstrated. In the time-lapse aerial photographs shown in figure 24, the 990 aircraft entered the slush-covered grooved concrete surface at an initial ground speed of 93.5 knots. With a 4-knot cross wind present and maximum antiskid braking being applied, the 990 aircraft maintained directional control on the runway center line on the slush-covered grooved concrete surface. The main-wheel velocity traces on the oscillograph record indicated no wheel lockup during this phase of the test run. However, when the aircraft entered the slush-covered ungrooved surface, main-wheel lockups did occur because of the abrupt reduction in the friction level provided by the runway surface. As a result of the

locked-wheel condition combined with the 4-knot cross wind, directional control of the 990 aircraft was not possible and the aircraft rotated into the wind, or weathercocked, as indicated in photograph 4 of figure 24.

The effect of runway grooves on the 990 aircraft main-wheel spin-up rate was also evaluated during a series of touch-and-go type tests on flooded grooved and ungrooved concrete (surfaces C and D). During these touchdown tests without braking a direct comparison of the main-wheel spin-up rates occurred during one test when the left main gear touched down first on the flooded grooved concrete and moments later the right main gear touched down on the adjacent flooded ungrooved surface. A time history of the outboard main-wheel velocity traces obtained during this test is shown in figure 25. The 990 aircraft was equipped with smooth main-gear tires during this test. As indicated by the wheel velocity traces (fig. 25), full main-wheel spin-up occurred in approximately 0.6 sec from touchdown on the flooded grooved section compared with approximately 0.9 sec on the flooded ungrooved section for the rear outboard wheel. The front outboard wheel on the right main gear, however, did not attain full spin-up until encountering a dry surface, a result which is indicative of the relatively low friction developed between the smooth tire and the flooded ungrooved surface. The path clearing of the surface water by the front tire resulted in the shorter spin-up time for the rear wheel on the right main gear than for the front wheel. The rapid wheel spin-up provided by runway grooves for flooded conditions is important in alleviating not only dynamic hydroplaning but also reverted rubber skids which occur during prolonged wheel lockups. (See ref. 9.)

Effect of runway surface water depth.- On the Gripstop (see ref. 7) transition section (surface E) having a length of 650 ft and a slope of 0.1 percent, aircraft braking test runs were conducted with just the lower half of the surface wet or flooded, leaving the upper half dry. During the braking tests on this surface, however, the wetness condition of the surface varied from a damp condition with no standing water to a deeply flooded condition with a water depth of 0.4 in. at the lower end of the surface. For these test-surface conditions, figure 26 shows a time history of main-wheel velocity and longitudinal accelerometer traces obtained during a high-speed maximum antiskid braking run with the 990 aircraft equipped with smooth tires. Maximum braking was obtained on the dry portion of the Gripstop test surface resulting in a 0.5g deceleration prior to the aircraft entering the damp surface area. As the 990 aircraft under maximum braking traveled through the damp area into the deeply flooded surface, braking effectiveness was reduced to near zero and numerous wheel lockups resulted. When brake release occurred as indicated in figure 26, the two forward wheels on the left main gear remained locked under hydroplaning conditions until encountering a dry, high friction level surface.

This hazardous locked-wheel condition, shown in figure 26 and discussed in references 3 to 6, results in complete loss of directional control or the inability of the tire to develop appreciable side force. The effect of this locked-wheel condition combined with a 12-knot cross wind which was present during the 990 aircraft braking test run on the Gripstop surface is shown in figure 27. The time-lapse photographs of the 990 aircraft were taken with a camera located at the end of the runway center line. The sequence of test-run events was as follows: (1) the aircraft entered the dry portion of surface E off the runway center line; (2) during maximum antiskid braking on the dry and the damp test areas of surface E, the pilot had directional control of the aircraft and was able to regain the runway center line (see photographs 1 and 2 in fig. 27); (3) upon entering the deeply flooded test area, numerous main-wheel lockups occurred (see fig. 26) which resulted in complete loss of aircraft directional control; and (4) the aircraft started to drift laterally off the runway center line (see photograph 4 in fig. 27). The severe lateral drifting of the 990 aircraft during this braking run with a 12-knot cross wind continued until the pilot released brakes and the aircraft encountered a dry high friction surface. With these hazardous conditions present on the entire length of an active ungrooved runway, safe aircraft landing operations would certainly be jeopardized.

Effect of tire tread design.- In past research work (see refs. 3 to 6), aircraft tire tread design has been shown to be an important factor in developing traction on wet or flooded ungrooved runway pavements. To evaluate further the effects of tire tread design, specially molded, smooth retread tires having new tire tread skid depths, as well as 5-groove rib-tread tires, were used during the 990 aircraft test program. A comparison of the aircraft braking data obtained with the 5-groove and the smooth tires on wet grooved and ungrooved concrete (surfaces C and D) is shown in figure 28. The dry braking friction coefficient level indicated in figure 28 did not vary significantly with tire tread design or surface configuration. For the wet ungrooved concrete, however, the 5-groove-tire data indicate a significant improvement in braking capability compared with the smooth-tire data. On the wet grooved concrete, the transverse runway grooves provided substantially greater braking friction levels with both tire tread designs than were shown by the data obtained on the wet ungrooved concrete. The data also indicate that runway grooves tend to minimize the effects of tire tread design and tire wear on braking friction capability.

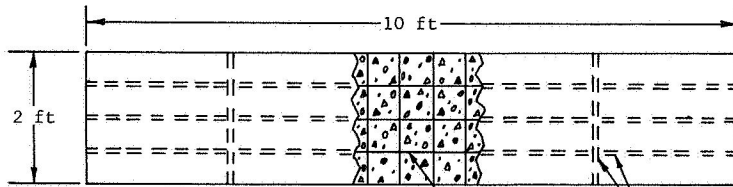
CONCLUDING REMARKS

The F-4D and the 990 aircraft braking test results obtained on dry, wet, flooded, and slush-covered grooved and ungrooved surfaces at the landing research runway at NASA Wallops Station have substantiated and supplemented the results obtained at the Langley landing-loads track. The comparative aircraft test results indicate that

transverse runway grooves provide (1) substantially increased aircraft braking capability and directional control, (2) improved runway surface water drainage, and (3) more rapid wheel spin-up rates. Runway grooves were also shown to minimize the effects of tire tread design or tire wear and the susceptibility to dynamic tire hydroplaning and reverted rubber skids. To obtain a complete evaluation of the effects of runway grooves on aircraft landing and take-off operations, more aircraft tests are planned at the landing research runway. The effects of traffic, loading, and weathering on grooved surface deterioration have yet to be determined although the test results obtained with the F-4D and 990 aircraft are very encouraging.

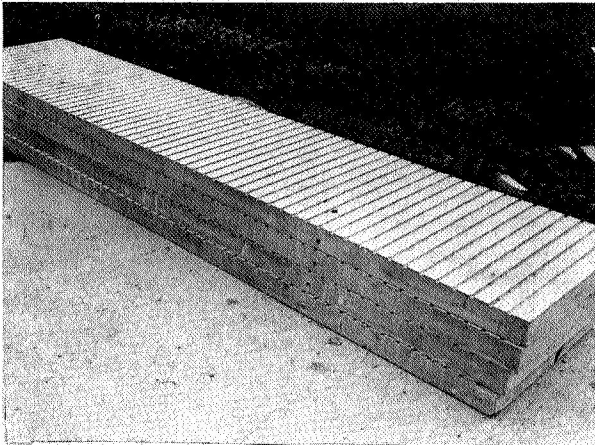
REFERENCES

1. Joyner, Upshur T.; and Horne, Walter B.: Considerations on a Large Hydraulic Jet Catapult. NACA TN 3203, 1954. (Supersedes NACA RM L51B27.)
2. Joyner, Upshur T.; Horne, Walter B.; and Leland, Trafford J. W.: Investigations on the Ground Performance of Aircraft Relating to Wet Runway Braking and Slush Drag. AGARD Rep. 429, Jan. 1963.
3. Horne, Walter B.; Yager, Thomas J.; and Taylor, Glenn R.: Review of Causes and Alleviation of Low Tire Traction on Wet Runways. NASA TN D-4406, 1968.
4. Leland, Trafford J. W.; Yager, Thomas J.; and Joyner, Upshur T.: Effects of Pavement Texture on Wet-Runway Braking Performance. NASA TN D-4323, 1968.
5. Horne, Walter B.; and Dreher, Robert C.: Phenomena of Pneumatic Tire Hydroplaning. NASA TN D-2056, 1963.
6. Horne, Walter B.; and Leland, Trafford J. W.: Influence of Tire Tread Pattern and Runway Surface Condition on Braking Friction and Rolling Resistance of a Modern Aircraft Tire. NASA TN D-1376, 1962.
7. Horne, Walter B.: Results From Studies of Highway Grooving and Texturing at NASA Wallops Station. Pavement Grooving and Traction Studies, NASA SP-5073, 1969. (Paper No. 26 herein.)
8. Anon.: Joint Technical Conference on Slush Drag and Braking Problems. FAA and NASA, Dec. 1961.
9. Nybakken, G. H.; Staples, R. J.; and Clark, S. K.: Laboratory Experiments on Reverted Rubber Friction. Tech. Rep. No. 7 (NASA Grant No. NsG-344), College Eng., Univ. of Michigan, Oct. 1968.

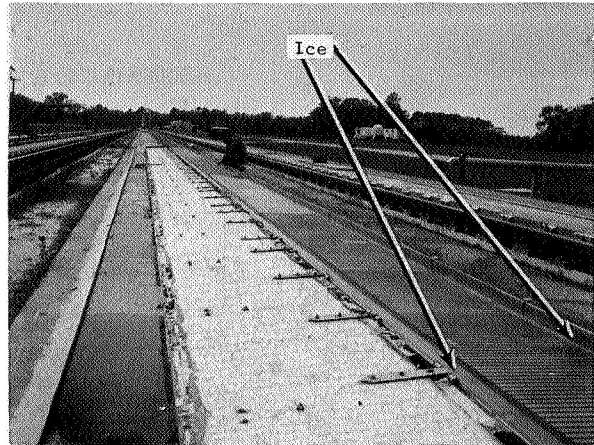


0.5-ft by 0.5-ft wire mesh at center of 0.25-ft depth — Steel reinforcement bars

(a) Plan drawing of precast concrete test strips.



(b) Grooved concrete strips before testing.



(c) Concrete strips installed in runway.

Figure 1.- Precast concrete test strips.

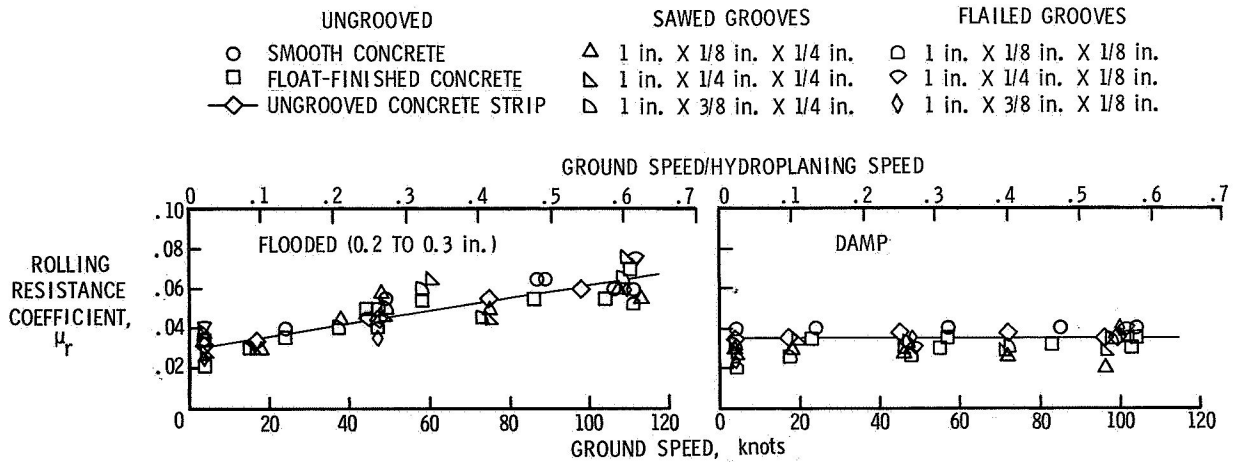
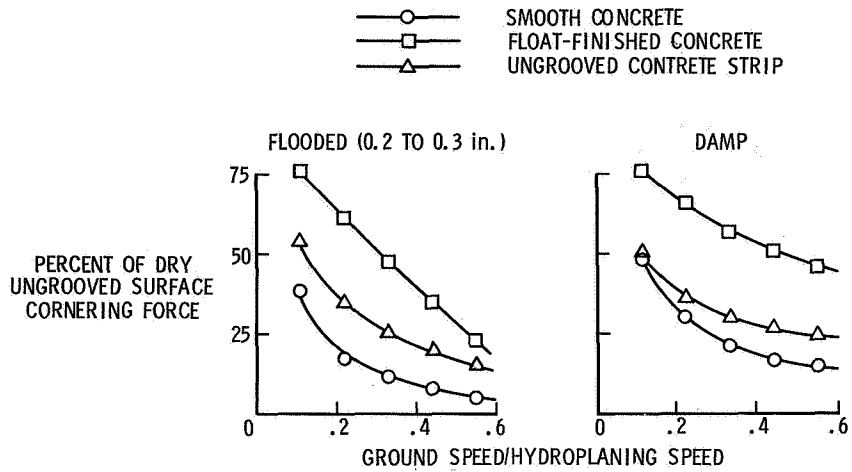
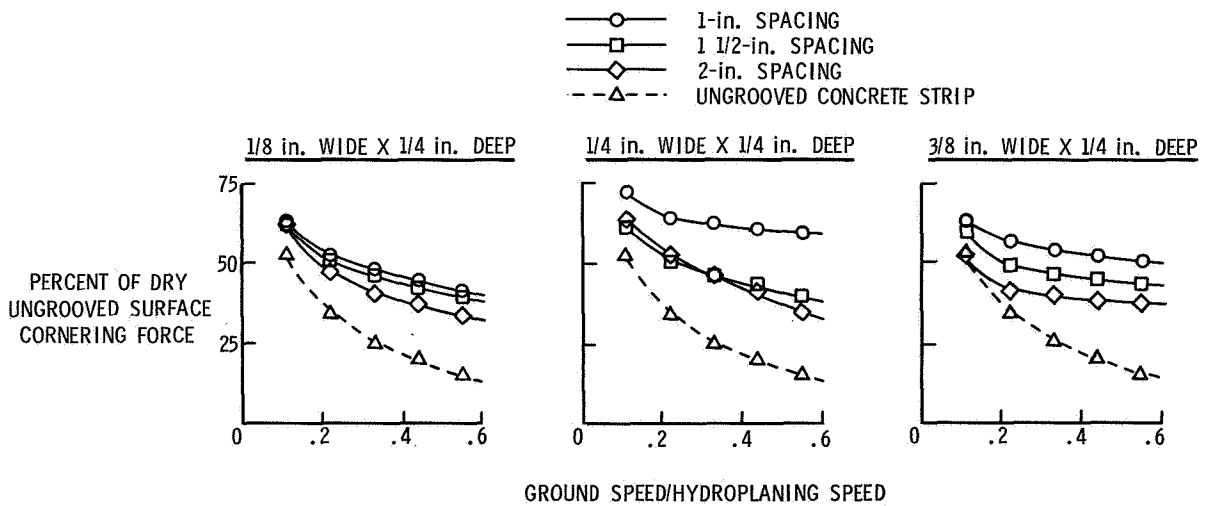


Figure 2.- Effect of runway wetness condition and surface configuration on rolling resistance of unbraked smooth, type VIII, 27.5 x 7.5 tire. Yaw angle, 4°; inflation pressure, 400 lb/in².

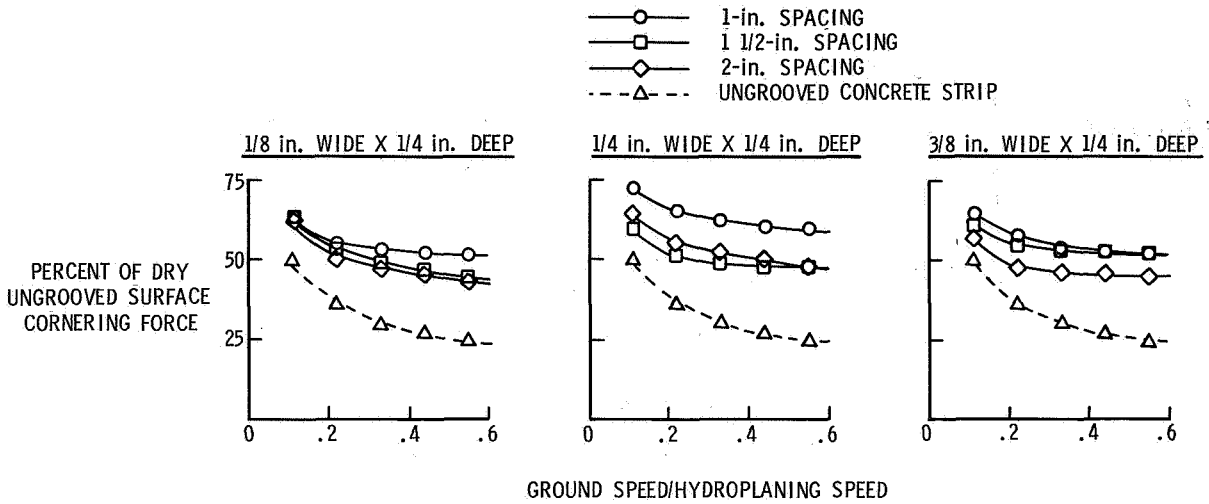


(a) Ungrooved surfaces.

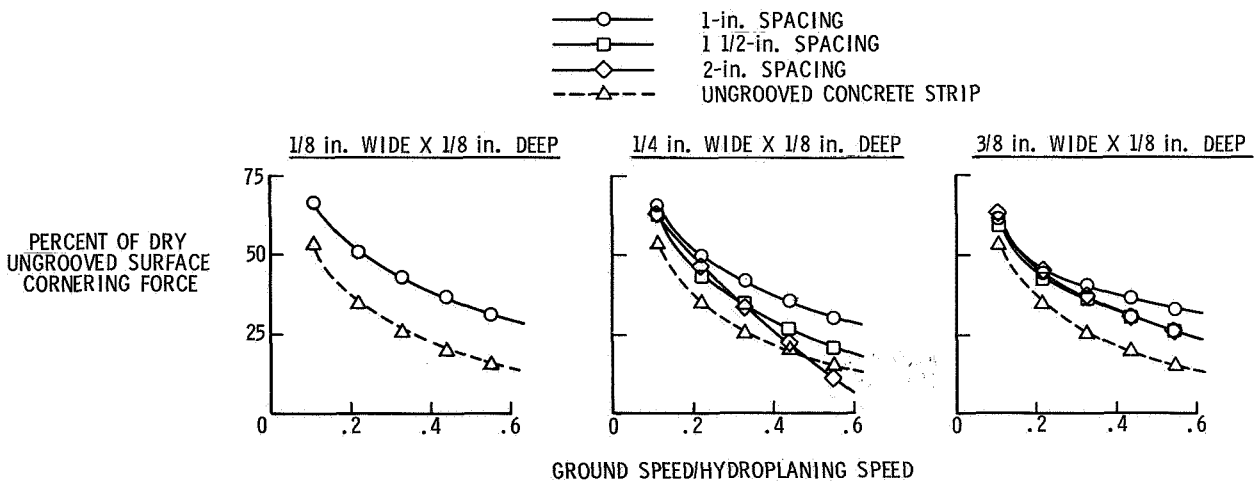


(b) Sawed grooves; flooded (0.2 to 0.3 in.).

Figure 3.- Effect of runway wetness condition and surface configuration on the cornering force of smooth, type VIII, 27.5 x 7.5 tire. Yaw angle, 4°; inflation pressure, 400 lb/in².

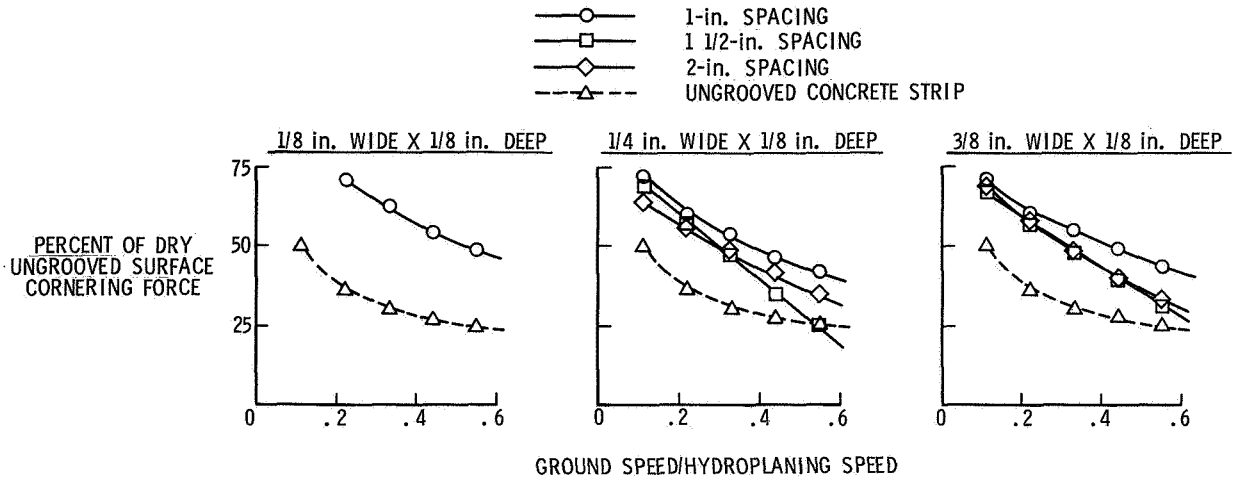


(c) Sawed grooves; damp.



(d) Flailed grooves; flooded (0.2 to 0.3 in.).

Figure 3.- Continued.



(e) Flailed grooves; damp.

Figure 3.- Concluded.

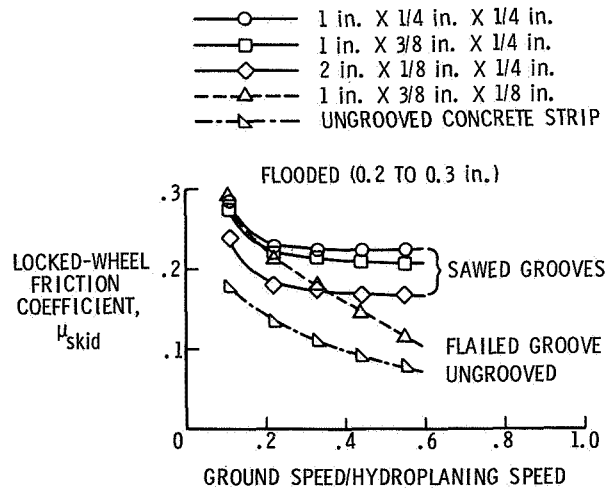


Figure 4.- Effect of runway surface configuration on locked-wheel friction coefficient of smooth, type VIII, 27.5 x 7.5 tire. Yaw angle, 4°; inflation pressure, 400 lb/in².

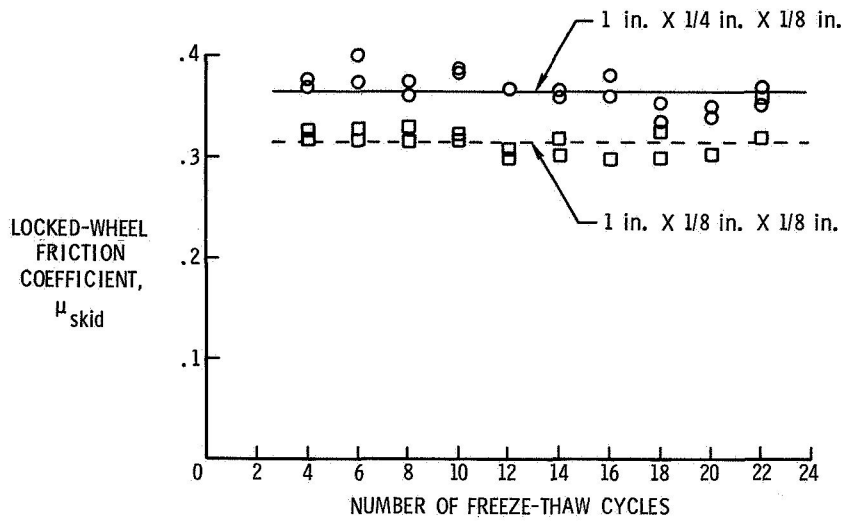


Figure 5.- Effect of alternately freezing and thawing flooded grooves on locked-wheel friction coefficient of 3-groove, type VIII, 30 x 11.5-14.5 tire. Yaw angle, 0°; inflation pressure, 210 lb/in²; ground speed, 4 knots.

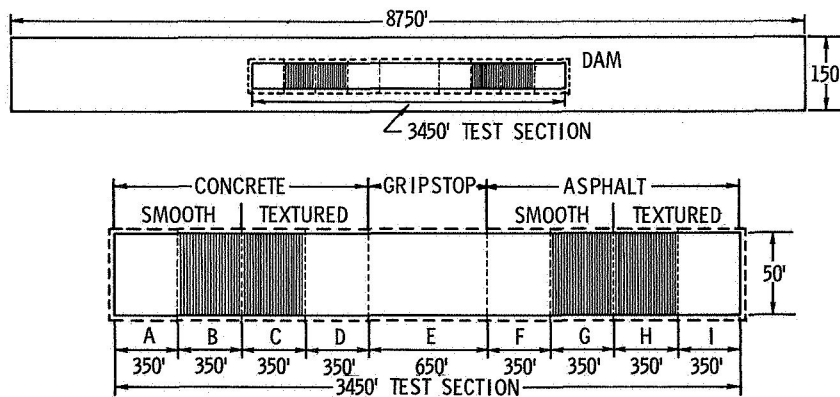
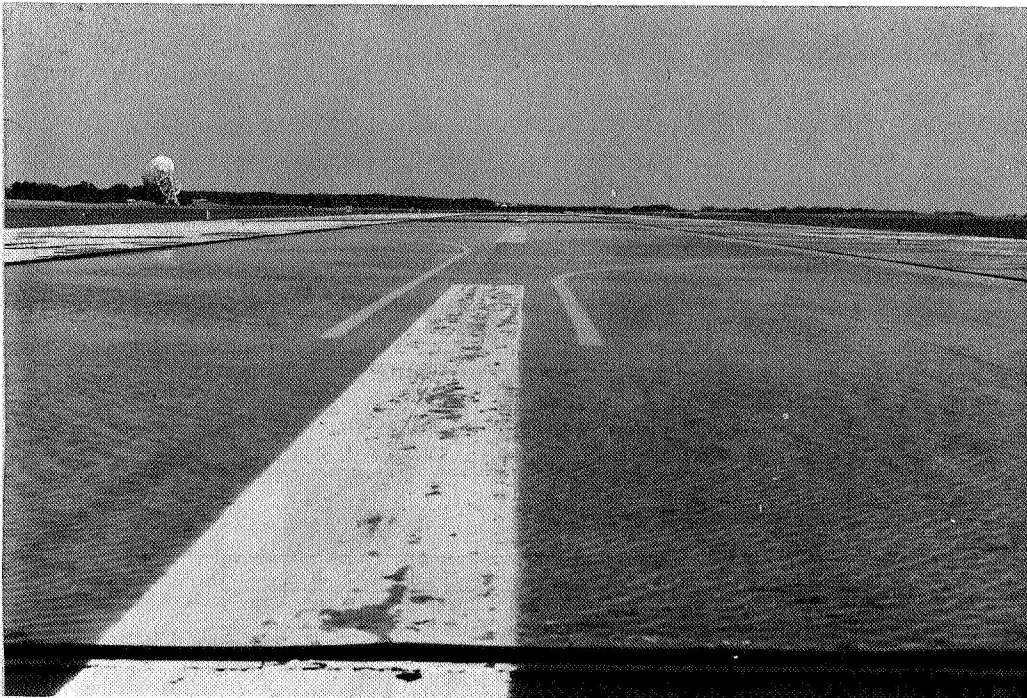


Figure 6.- Landing research runway at NASA Wallops Station.



(a) Wet with isolated puddles.



(b) Flooded.

Figure 7.- Surface wetness conditions on landing research runway.

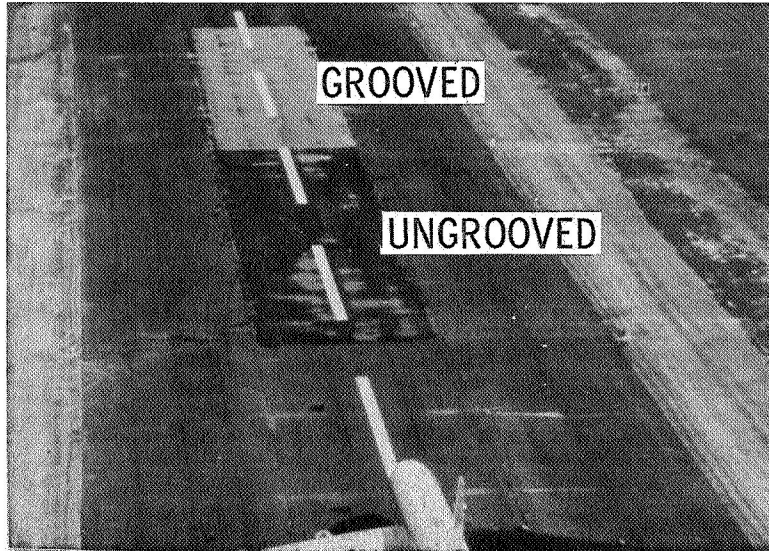


Figure 8.- Effect of runway grooves on water drainage.

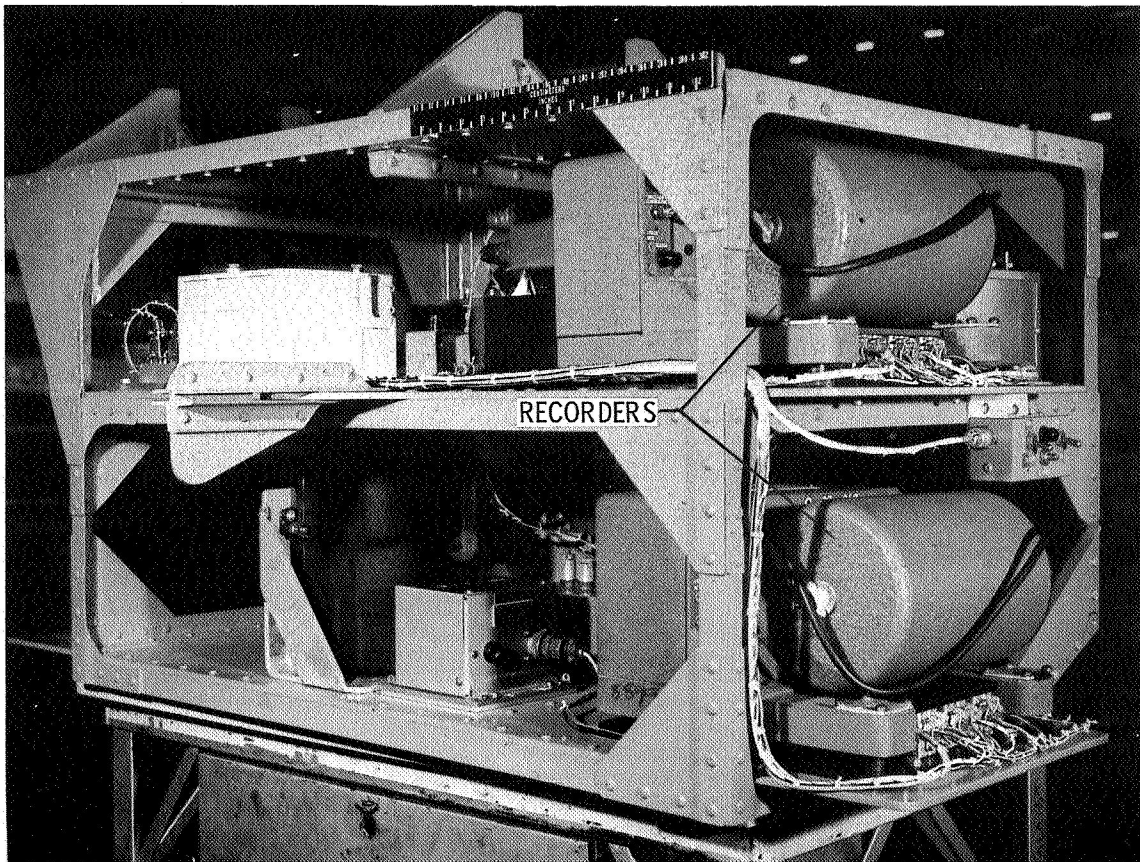


Figure 9.- Onboard instrument package for aircraft tests.

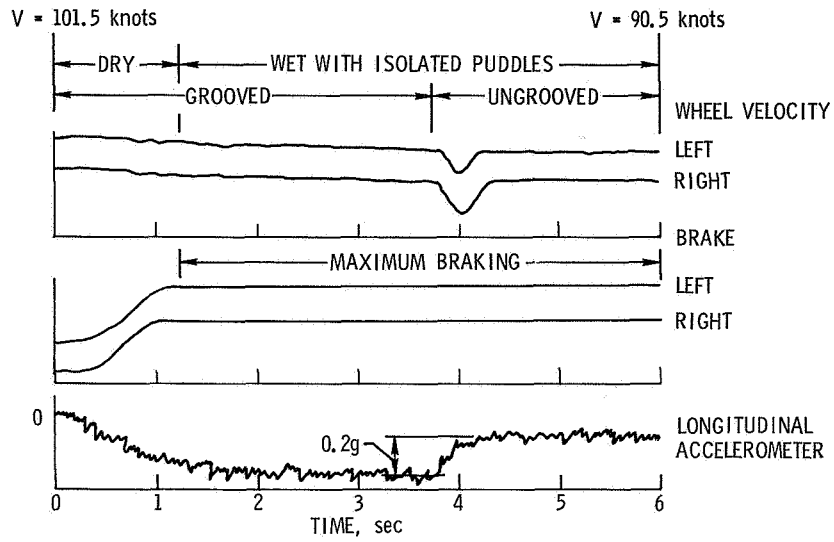


Figure 10.- Effect of wet grooved and ungrooved surfaces on F-4D aircraft braking. 3-groove tires; inflation pressure, 280 lb/in²; concrete.

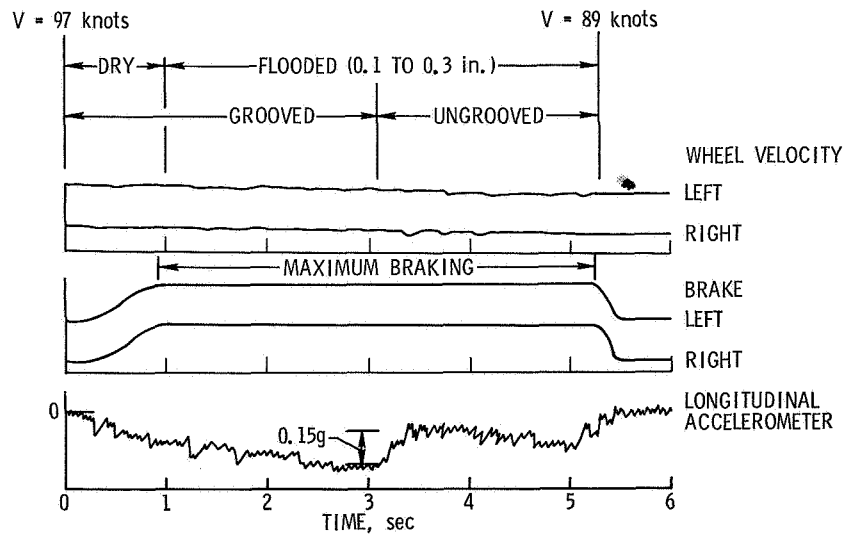


Figure 11.- Effect of flooded grooved and ungrooved surfaces on F-4D aircraft braking. 3-groove tires; inflation pressure, 280 lb/in²; concrete.

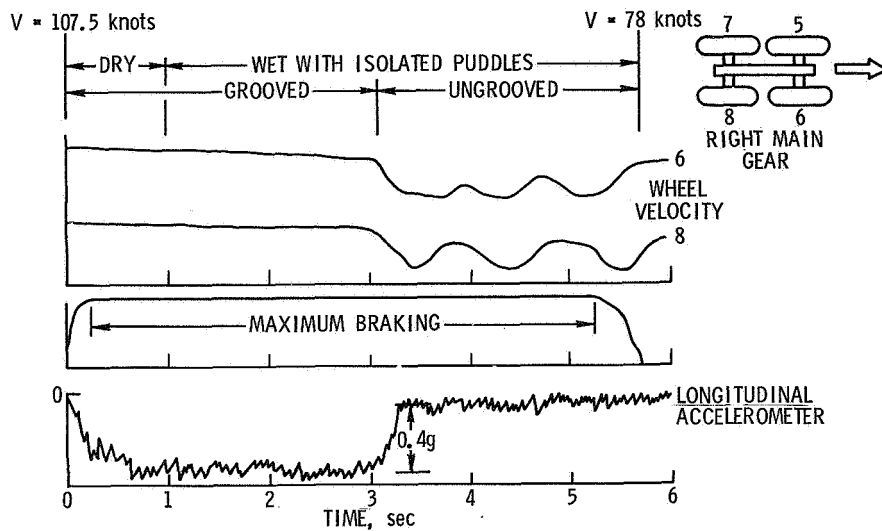


Figure 12.- Effect of wet grooved and ungrooved surfaces on 990 aircraft braking. Smooth tires; inflation pressure, 160 lb/in²; concrete.

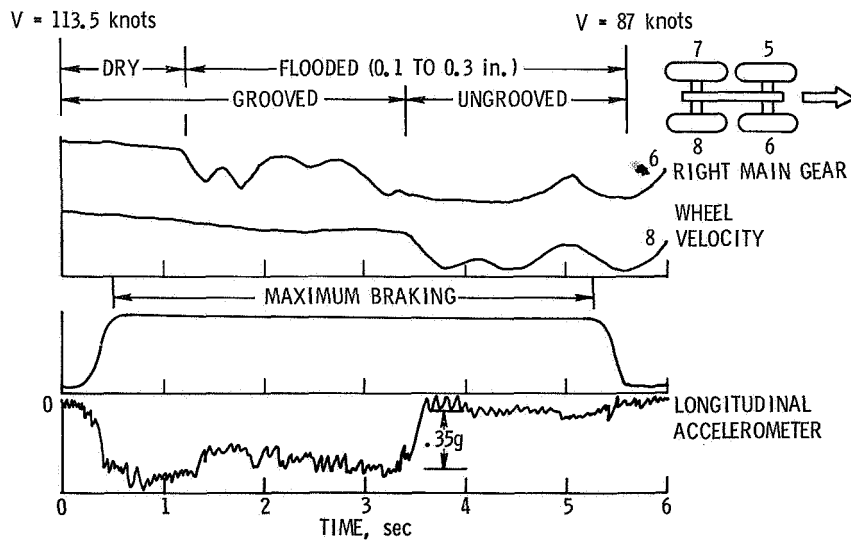


Figure 13.- Effect of flooded grooved and ungrooved surfaces on 990 aircraft braking. Smooth tires; inflation pressure, 160 lb/in²; concrete.

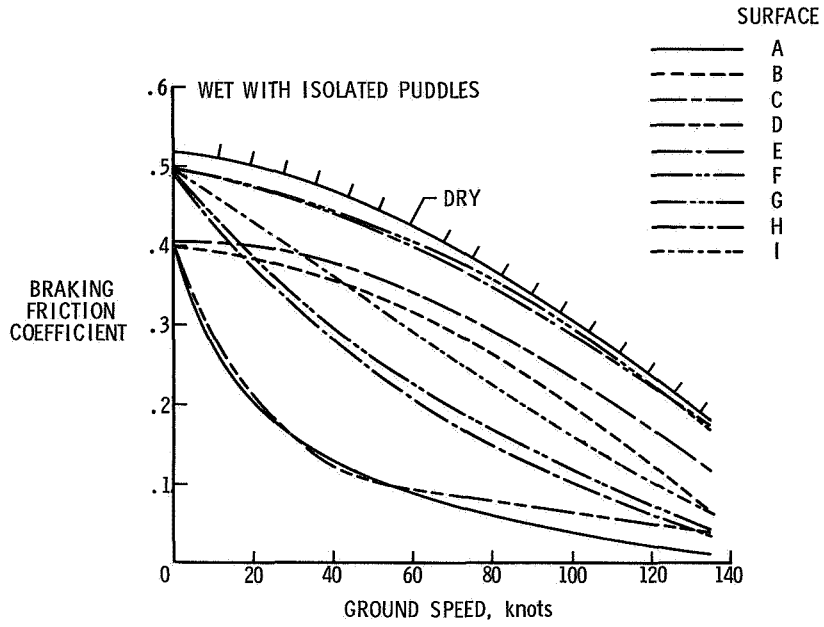


Figure 14.- Variation of F-4D aircraft braking friction coefficient with ground speed on wet grooved and ungrooved surfaces. 3-groove, type VIII, 30 × 11.5-14.5 main tires; inflation pressure, 280 lb/in².

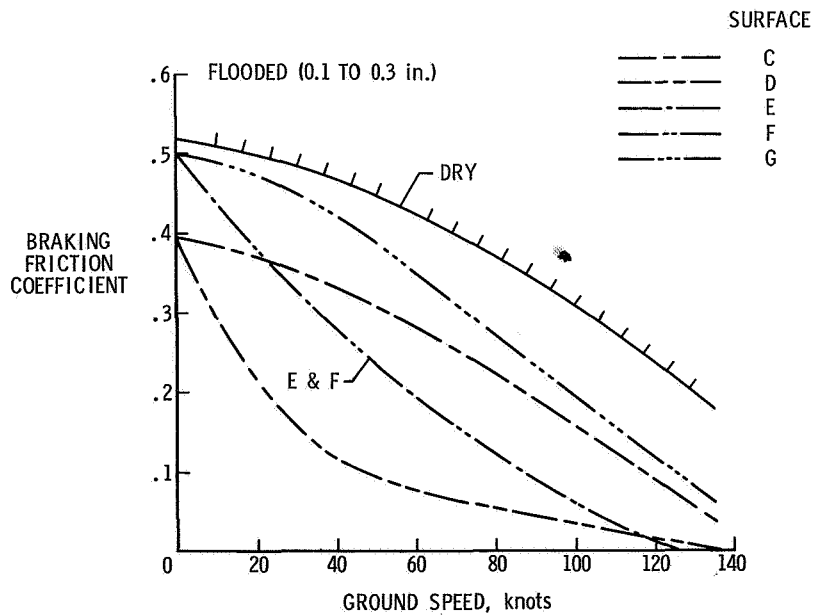


Figure 15.- Variation of F-4D aircraft braking friction coefficient with ground speed on flooded grooved and ungrooved surfaces. 3-groove, type VIII, 30 × 11.5-14.5 main tires; inflation pressure, 280 lb/in².

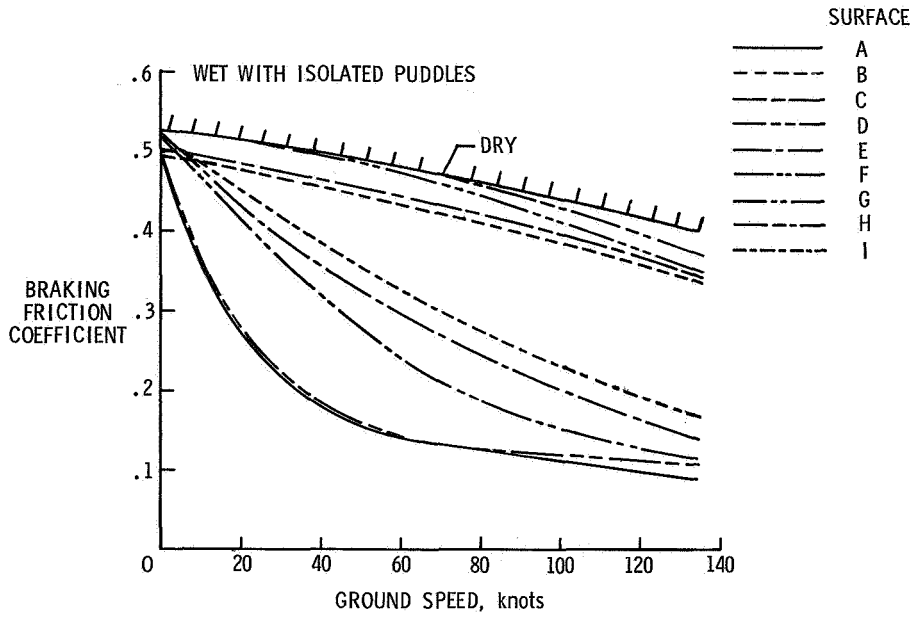


Figure 16.- Variation of 990 aircraft braking friction coefficient with ground speed on wet grooved and ungrooved surfaces. 5-groove, type VIII, 41 × 15.0-18 main tires; inflation pressure, 160 lb/in².

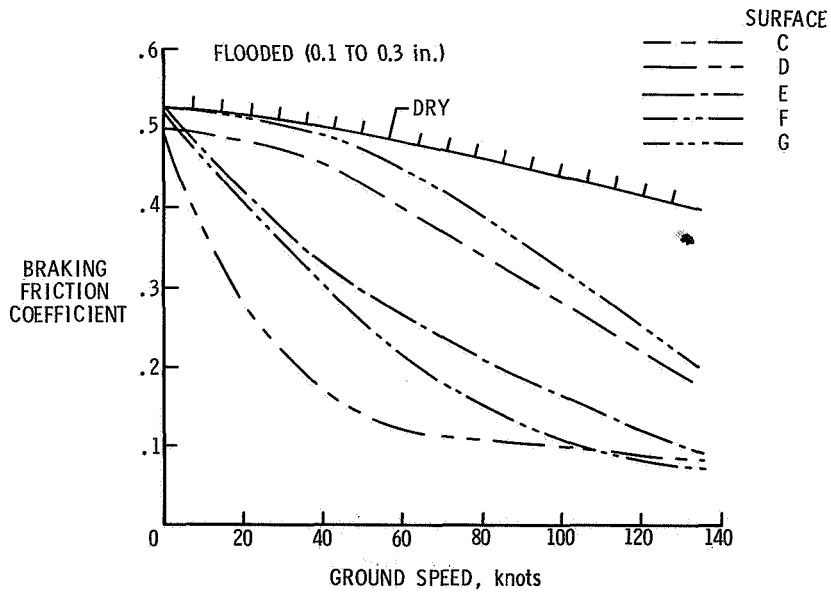


Figure 17.- Variation of 990 aircraft braking friction coefficient with ground speed on flooded grooved and ungrooved surfaces. 5-groove, type VIII, 41 × 15.0-18 main tires; inflation pressure, 160 lb/in².

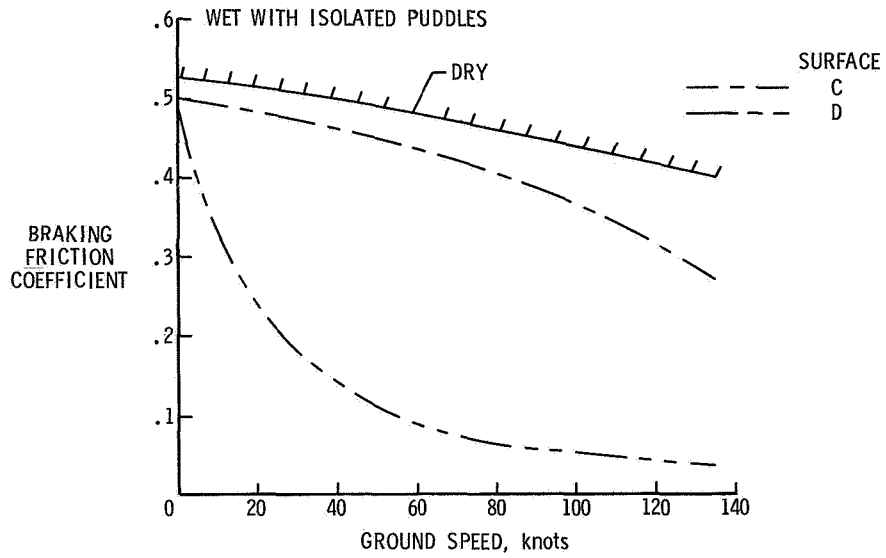


Figure 18.- Variation of 990 aircraft braking friction coefficient with ground speed on wet grooved and ungrooved surfaces. Smooth, type VI,II, 41 × 15.0-18 main tires; inflation pressure, 160 lb/in².

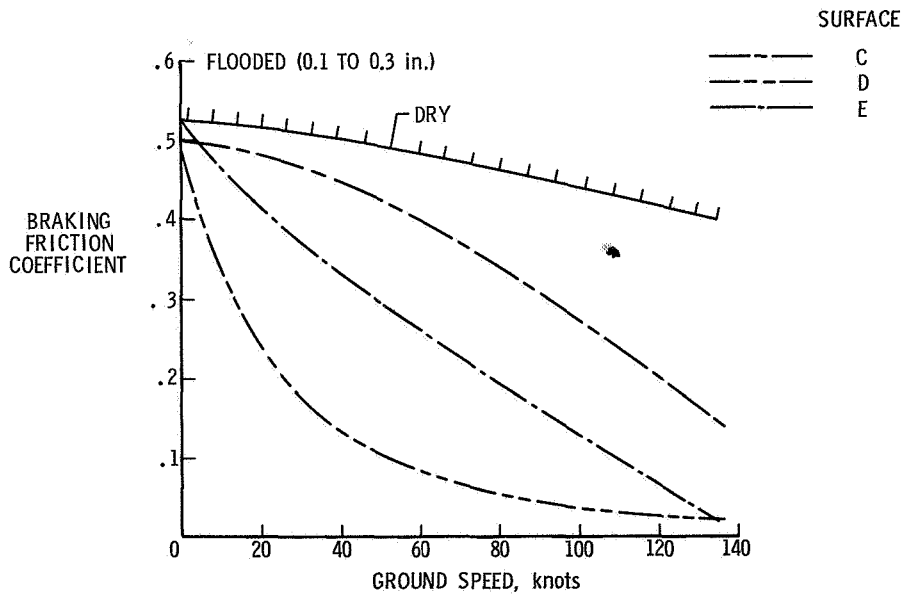


Figure 19.- Variation of 990 aircraft braking friction coefficient with ground speed on flooded grooved and ungrooved surfaces. Smooth, type VIII, 41 × 15.0-18 main tires; inflation pressure, 160 lb/in².

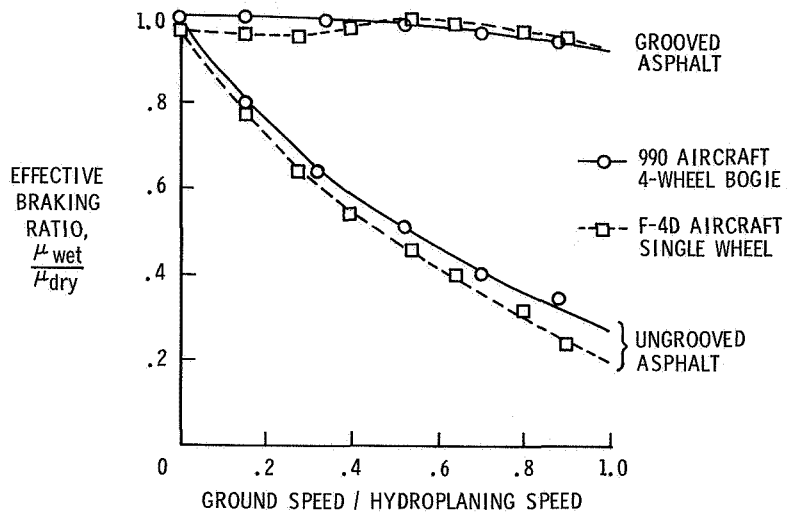


Figure 20.- Effect of runway grooves on aircraft braking performance. Wet with isolated puddles.

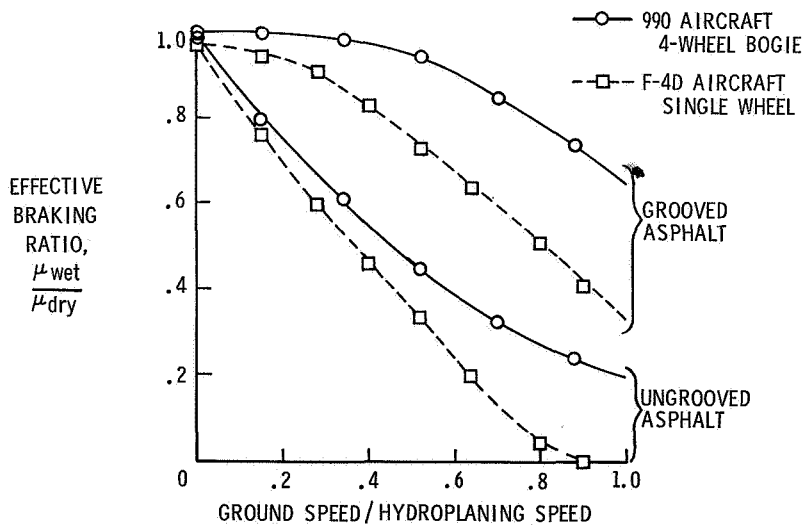


Figure 21.- Effect of runway grooves on aircraft braking performance. Flooded (0.1 to 0.3 in.).

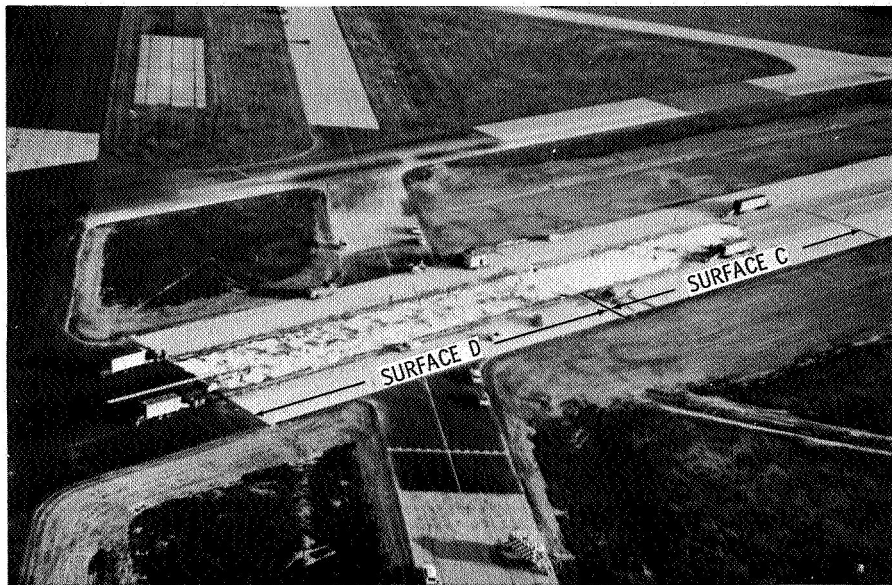


Figure 22.- Slush-covered runway surface condition.

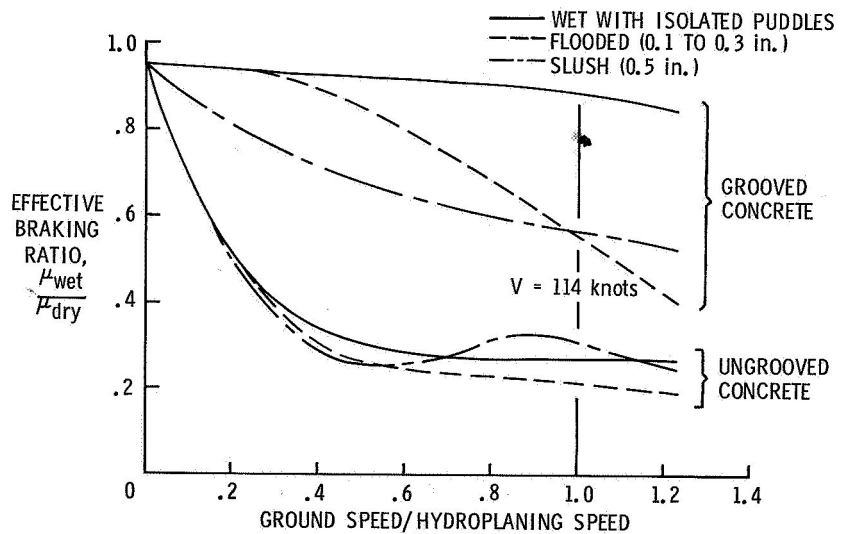


Figure 23.- Effect of runway grooves on 990 aircraft braking performance. 5-groove tire; inflation pressure, 160 lb/in².

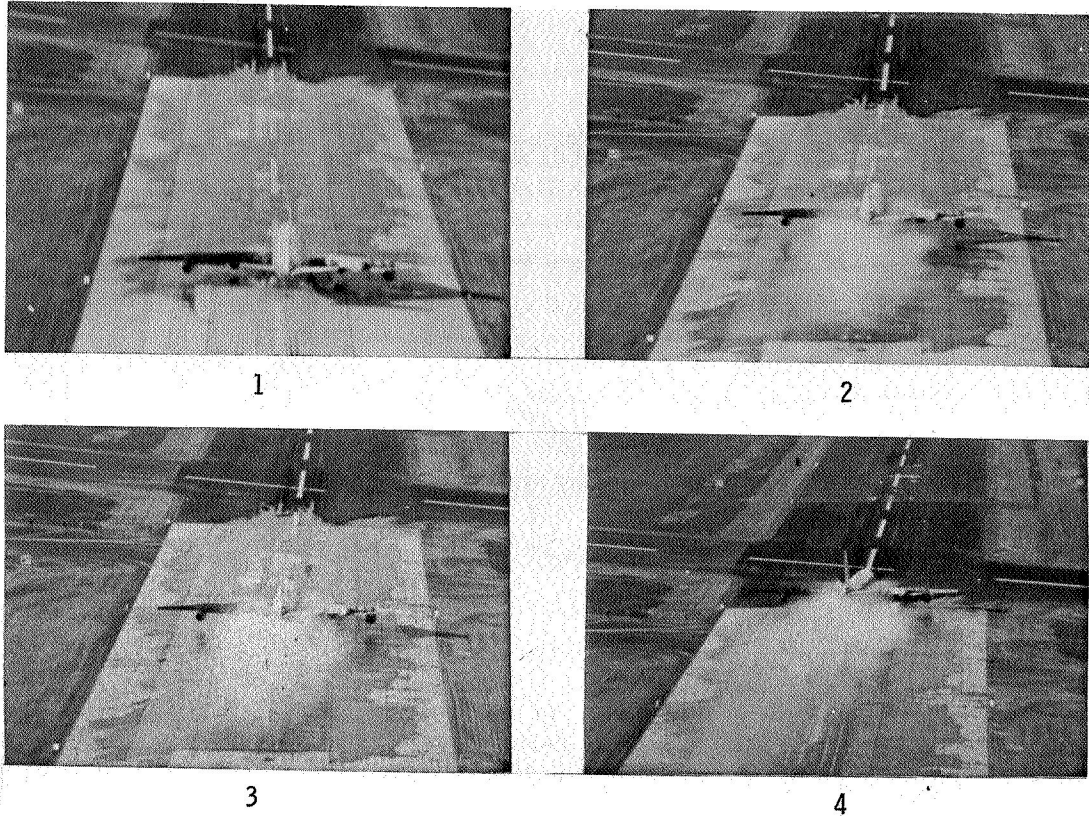


Figure 24.- Effect of slush-covered runway grooves on directional control of 990 aircraft. Cross wind, 4 knots.

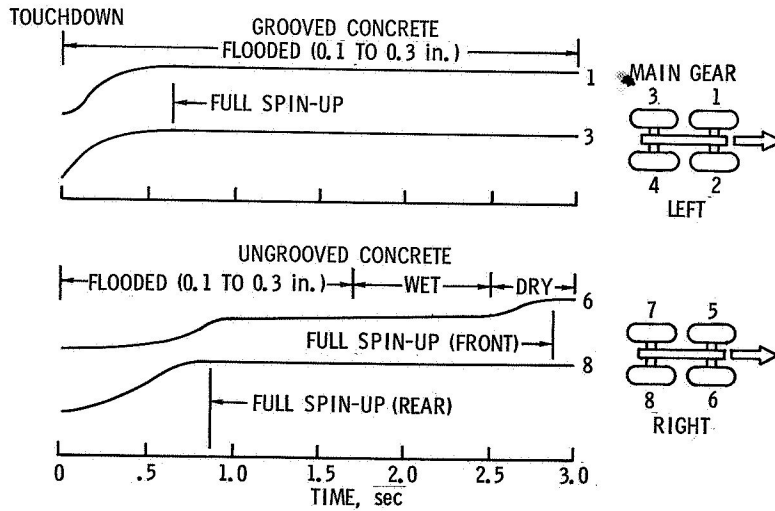


Figure 25.- Effect of runway grooves on 990 aircraft main-wheel spin-up rate. Smooth tires; inflation pressure, 160 lb/in².

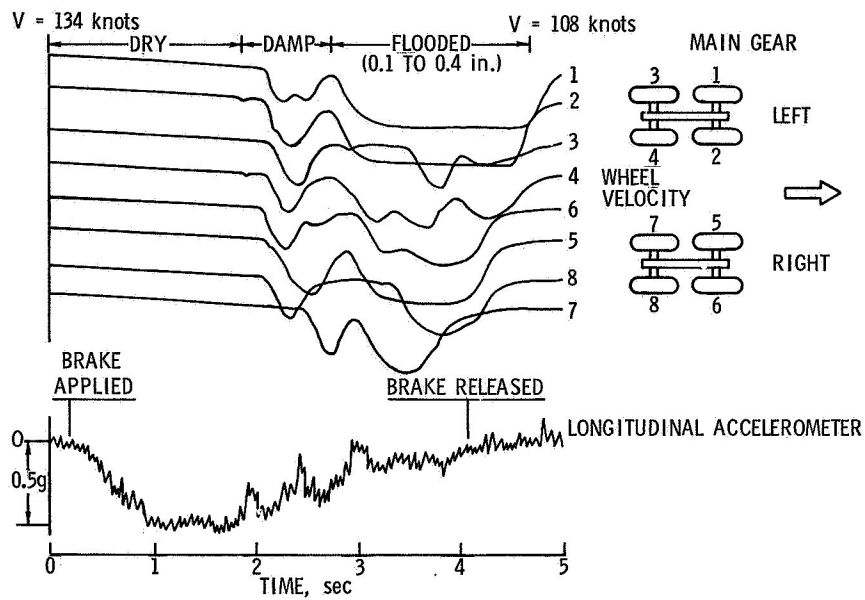


Figure 26.- Effect of water depth on 990 aircraft braking performance. Smooth tires; inflation pressure, 160 lb/in²; Gripstop; cross wind, 12 knots.

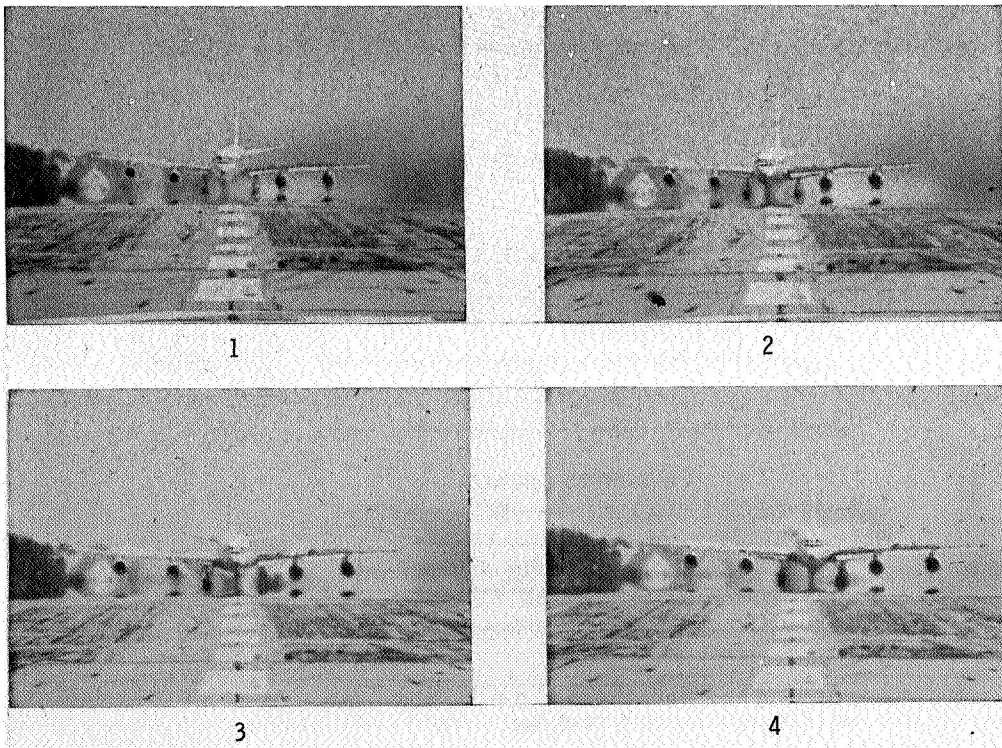


Figure 27.- Loss of directional control of 990 aircraft during braking test run on Gripstop. Cross wind, 12 knots.

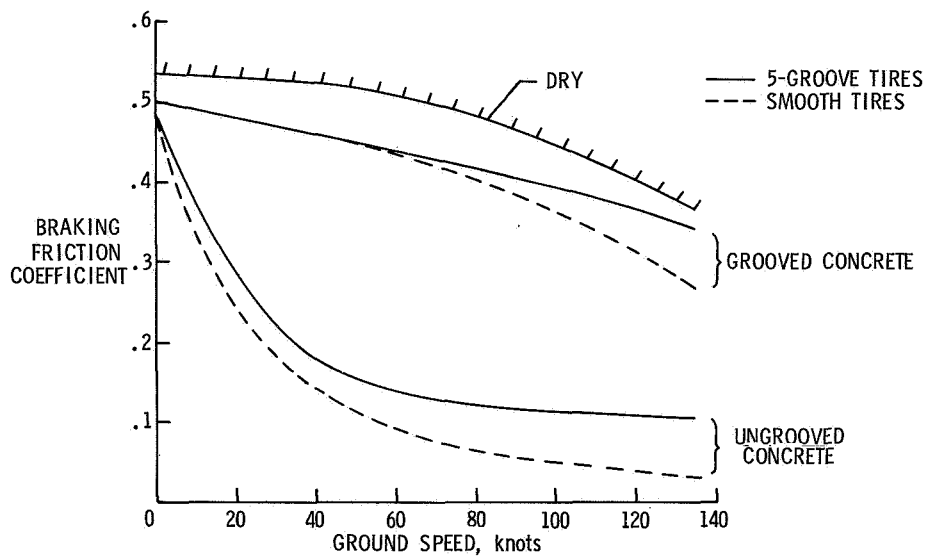


Figure 28.- Effect of tire tread design on 990 aircraft braking friction coefficient. Wet with isolated puddles.